Eur Biophys J (2011) 40:1143–1155
DOI 10.1007/s00249-011-0745-9

ORIGINAL PAPER

Structure of a protein–detergent complex: the balance between detergent cohesion and binding

Jonathan Khao · Jaime Arce-Lopera · James N. Sturgis · Jean-Pierre Duneau

Received: 17 March 2011 / Accepted: 10 August 2011 / Published online: 8 September 2011

Abstract Despite the major interest in membrane proteins at functional, genomic, and therapeutic levels, their biochemical and structural study remains challenging, as they require, among other things, solubilization in detergent micelles. The complexity of this task derives from the dependence of membrane protein structure on their anisotropic environment, influenced by a delicate balance between many different physicochemical properties. To study such properties in a small protein–detergent complex, we used fluorescence measurements and molecular dynamics (MD) simulations on the transmembrane part of glycophorin A (GpAtm) solubilized in micelles of dihexanoylphosphatidylcholine (DHPC) detergent. Fluorescence measurements show that DHPC has limited ability to solubilize the peptide, while MD provides a possible molecular explanation for this. We observe that the detergent molecules are balanced between two different types of interactions: cohesive interactions between detergent molecules that hold the micelle together, and adhesive interactions with the peptide. While the cohesive interactions are detergent mediated, the adhesion to the peptide depends on the specific interactions between the hydrophobic parts of the detergent and the topography of the peptide dictated by the amino acids. The balance between these two parameters results in a certain frustration of the system and rather slow equilibration. These observations suggest how molecular properties of detergents could influence membrane protein stabilization and solubilization.

J. Khao · J. Arce-Lopera · J. N. Sturgis · J.-P. Duneau (✉)
Laboratoire d'Ingénierie des Systèmes Macromoléculaires, CNRS—Aix Marseille Université, 31 Chemin Joseph Aiguier, 13402 Marseille cedex 20, France
e-mail: duneau@ifr88.cnrs-mrs.fr

Keywords FRET · Molecular dynamics simulations · Protein–detergent complex · Dihexanoylphosphatidylcholine · Glycophorin A

Introduction

Biological membranes and the integral membrane proteins they contain are responsible for a wide variety of biological processes. Genomic studies during the past decades have revealed that ~30% of genes are expected to code for membrane proteins (Wallin and von Heijne 1998). Moreover, 50–60% of drugs currently on the market target membrane proteins, and account for 25 of the best selling drugs (Drews 2000). Although membrane proteins are of major biological and medical interest, they remain relatively poorly studied; for example, only 2% of PDB entries are membrane proteins.

Biochemical and structural studies of membrane proteins are necessary steps towards understanding of these proteins, however such studies require protein solubilization using detergents. This is a particularly difficult process, and is often the limiting step in the study of membrane proteins. The complexity of membrane protein solubilization arises from the dependence of their structure and function on the lipid environment in the membrane. These proteins have evolved to be particularly well adapted to this anisotropic and chemically complex environment that contains a mixture of a great variety of lipids, each with different physicochemical properties and capable of influencing protein structure and function. It has been shown in several systems that lipids can play a key role in the properties of membrane proteins (Dowhan and Bogdanov 2009). Furthermore, the lipids present in a membrane are exceptionally diverse with many different molecular species present. The combination

of this diversity with the importance of the lipid environment for function and structure makes finding molecules able to render the system water soluble challenging. Thus, membrane protein solubilization remains critical and limits many studies on membrane proteins.

Maintaining membrane protein structure intact while changing the environment from a biological membrane to a solubilized system is delicate and usually involves the use of detergent micelles which have a hydrophobic core and a polar surface (Hauser 2000; Kessi et al. 1994). However, in view of the chemical diversity of detergents, choosing one capable of maintaining structure and function is difficult and time consuming, especially as it is not certain that such a detergent exists. Currently, detergent choice is usually based on laborious and empirical methods, such as experience from previous studies, perceived chemical harshness of the detergent, detergent fluidity, complex size, or cost. Therefore, attempts are numerous and costly screenings are required (Duquesne and Sturgis 2010; Garavito et al. 1996). Associated with these difficulties is the small and poorly characterized difference in physicochemical properties between the surface of the transmembrane helical bundle and the interior of the protein (Rees et al. 1989). As solubilization requires sufficient detergent binding to membrane hydrophobic surfaces, it is often difficult to prevent an interaction with the protein interior that will denature the protein. This difficulty in discrimination between surface and interior is thought to be a major source of so-called detergent aggressiveness (Breyton et al. 2010; Tate 2010). Because of the subtlety of the interactions between a detergent and the different parts of a membrane protein, it is important to understand at a molecular level the nature of these interactions, and the molecular parameters that can modulate detergent–protein interactions.

To this end, our group has previously experimentally studied the dependence of transmembrane peptide association on detergent nature and concentration (Fisher et al. 2003). We observed that the detergent concentration effect on the dimerization of the single transmembrane domain of glycophorin A (GpAtm) was not only entropy dependent, as might be predicted from a simple solubilization–dilution model. From this observation it was hypothesized that the interactions of detergent molecules with the distinct faces of GpAtm were not equivalent. Furthermore, the thermodynamic behavior could be best explained with a model in which a distinct peptide–detergent complex (PDC) changes to a structure more closely resembling a dimer solubilized within a detergent micelle. To date no structural information is available to support these hypotheses, and indeed very little is known about the structure of any PDC.

Tools such as molecular dynamics simulation can provide atomic-resolution vision of simple chemical systems. From such vision it is possible to extract information about the structure, the dynamics, and the forces that control the structure of the studied system (van Gunsteren and Berendsen 1984). Therefore, as an extension of our former experimental studies, we describe molecular dynamics simulations of a PDC formed by GpAtm and the dihexanoylphosphatidylcholine (DHPC) detergent which we compare with experimental measurements of the same system. DHPC is a versatile detergent which is gaining interest for structural studies of membrane proteins, in crystallography, and in both liquid- and solid-state nuclear magnetic resonance (NMR). It is a lipid molecule from which detergent properties arise from its short acyl chains (Chou et al. 2004; Fernández et al. 2004; Hauser 2000; Kessi et al. 1994; Sanders and Sönnichsen 2006; Tausk 1974).

Our simulations suggests that the PDC formed by GpAtm and DHPC is a relatively rigid structure in which the different surfaces of GpAtm interact in distinct manners with the detergent. In particular, we note that the rotation of the peptide relative to the micelle is restricted and, in agreement with the previous experimental analysis, that the dimerization motif interacts only weakly with the various detergents.

Furthermore, we observe that the peptide has a tendency to expose some of its hydrophobic surfaces to the aqueous solvent. This is in agreement with the Förster resonance energy transfer (FRET) results showing that higher-order GpAtm oligomers can be observed well above the detergent critical micelle concentration (CMC).

Materials and methods

Fluorescence measurements

Peptides corresponding to the sequence of the human glycophorin A transmembrane domain (residues 69–101) were synthesized and purified as described previously (Fisher et al. 1999). The peptides were labeled with a donor (pyrene) or with an acceptor 7-(*N*,*N*-dimethylamino)-coumarin at the amino terminus (Fisher and Engelman 2001; Fisher et al. 1999, 2003). Lyophilized peptides were reconstituted in 25 mM Na phosphate buffer pH 7.4, 0.2 M NaCl, with the DHPC detergent (Avanti Polar Lipids) at the specified concentrations. All fluorescence spectra were recorded on a Fluorolog 3–21 photon counting spectrofluorimeter (Spex, Longjumeau, France) equipped with a 450 W xenon source, an additive double excitation monochromator, a single emission monochromator, and a cooled photomultiplier. Förster resonance energy transfer (FRET) between pyrene- and coumarin-labeled GpA peptides was measured as previously described (Fisher et al. 1999, 2003). Briefly, the assay was developed to provide a sensitive measure of

transmembrane peptide association that is relatively insensitive to the details of the peptide–detergent complex. Fluorescence excitation spectra were recorded and corrected for the direct emission of the fluorophores. The relative contribution of pyrene and coumarin to the fluorescence emission at 500 nm was calculated. This ratio (FRET ratio) provides a sensitive measure of the degree of dimerization in diverse environments.

MD system setup

The S24 complex structure was built from a micelle simulation with 27 detergent monomers that aggregated from dispersed detergent molecules; the micelle was equilibrated over 20 ns. Three detergent molecules were removed to allow insertion of the GpA peptide (residues 71–96) in a "transmicelle" orientation. The hydrated system was minimized using steepest descent and conjugate gradient methods, and then heated from the 0 K minimized configuration to 298 K using a Berendsen thermostat (Berendsen et al. 1984) and strong coupling to the thermal bath. In the early stages of equilibration a spontaneous tilting of the peptide was observed, leading to an orientation parallel to the plane of the bilayer-like micelle in the middle of the hydrocarbon core of the DHPC aggregate. In this configuration, the hydrophobic part of the transmembrane peptide remains buried from the water solvent whereas the hydrophilic extremities of the peptide protrude laterally from the complex, being fully exposed to the aqueous environment. This orientation was maintained throughout the simulations.

Molecular dynamics simulations

Molecular dynamics simulations were performed with the GROMACS 3.3.1 software package (Van Der Spoel et al. 2005) using the G45A3 force field (Soares et al. 2004), specially parametrized for phosphatidyl-choline lipids, and the simple point charge water model (Berendsen et al. 1981) in an *NPT* ensemble. The system was maintained at constant temperature of 298 K using the Berendsen thermal bath with time constant of 0.1 ps. The pressure was held to 1 bar using the Berendsen isotropic algorithm with time constant of 1 ps. Lincs (Hess et al. 1997) was used to constrain bond lengths, allowing a 2-fs time step. Long-range electrostatic interactions were computed using the particle mesh Ewald method (Darden et al. 1999) with grid spacing of 1.2 A, optimized by GROMACS and fourth-order spline interpolation. van der Waals interactions were truncated at 1.2 nm. From the 20th ns of S24 and the first frame of S24R, dihedral angle constraints on the helix backbone were used to maintain the canonical structure, using force constraints of 100 kJ mol^{-1} rad^{-2}. The GpA dimer was maintained using harmonic bonds with force constant of 100 kJ mol^{-1} nm^{-2} between residue center of mass, when interchain distance restraints were available from NMR. Detergent number varied from 24 to 17 over the different GpA monomer simulations (Fig. 2, see below for details) and was fixed to 48 for the GpA dimer simulation. NaCl concentration was set to 100 mM, which corresponded to 17 ions, and a total of $\sim$10,000 water molecules were added to fill the box.

Ptuba projections

Figures 7 and 8 were generated using projection of transmembrane helices using a uniform B-spline algorithm (Ptuba) (Lopera et al. 2005) representations. Briefly, Ptuba generates projections of helix surfaces, no matter what their deviations from a canonical helix might be. Surfaces are repeated twice to avoid discontinuities on edges. The projection allows simultaneous visualization of all the helix surfaces, which can be colored according to structural or interaction properties.

Results

Experimental dissociation of GpAtm in DHPC detergent

The FRET assay, previously used to characterize the dissociation ability of various detergents with transmembrane helices (Duneau et al. 2007; Fisher et al. 1999, 2003), was applied to GpAtm in DHPC. Figure 1 shows the results for peptide concentration ranging from 666 to 50 nM and detergent concentration from 14 mM (the CMC) to 200 mM. Our previous studies have shown that FRET ratio of 0.75 corresponds to the situation when the GpAtm is 100% dimeric. Higher values are due to the presence of higher-order oligomers. Our data were analyzed in the framework of two popular models that describe the effects of detergent on the apparent dissociation constant (Fisher et al. 2003; Fleming 2002). The first argues that Kd^0_{App} is simply proportional to the number of available micelles. The second assumes that some nonideal behavior can arise when excess detergent is released or mobilized following peptide dissociation. The fitting of the 666 nM data with the former model in the range of 40–200 mM DHPC (continuous line) gives an apparent Kd^0_{App} of 10.62 $\pm$ 0.65 μM. Using this value for Kd^0_{App} the predictions for other detergent concentrations (dotted and dashed lines) give very good agreement between the experiment and the model. This shows that it is unnecessary to take nonideal behavior into account in this system. This is also consistent with the treatment by Fisher et al. (2003) (inset) showing the linear relationship that exists between the apparent free energy of dissociation and the

logarithm of the detergent micellar concentration. The observed slope of -5.65 ± 0.46 is very close to the corresponding ideal value of -5.74. The second parameter, the free energy of dissociation standardized at 1 M micellar detergent concentration, is 28.11 ± 0.65 kJ mol^{-1}, a value which classifies DHPC as a mild detergent at 1 M concentration (similar to decyl maltoside), in this context. The slope also classifies this detergent as mild (favoring association) at low detergent concentrations.

In contrast to its behavior above 40–50 mM, an original feature of the DHPC detergent is the presence of higher-order peptide oligomers at detergent concentrations that are lower but still well above the CMC. This can be seen in Fig. 1, where the observed FRET ratio departs from the fits to reach values as high as 1 at detergent concentrations close to the CMC. For other detergents, similar aggregation behavior is only observed when the detergent concentration falls below the CMC. Based on these experiments, it appears that there is an unusual relationship between GpAtm and DHPC. To study this at a structural level, we used molecular dynamic simulations of both the monomer and the dimer of GpAtm. These results are presented in the following sections, and their relevance to the experimental findings is highlighted in the "Discussion."

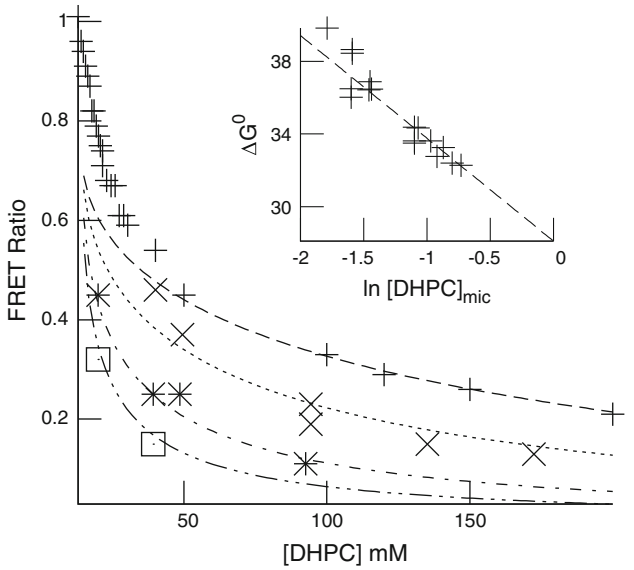

Fig. 1 FRET measurements of glycophorin A dissociation in DHPC detergent. The FRET ratio of labeled transmembrane domains of GpAtm at various concentrations (666 nM: *plus*; 300 nM: *cross*; 100 nm: *star*; 50 nM: *square*) was measured against increasing concentration of DHPC from 14 to 200 mM. *Lines* represent a fit against the model assumed in Flemming (2002) where the single fitted parameter corresponds to the dissociation constant at 1 M detergent (Kd^0). Only the 666 nM series from 50 to 200 mM DHPC was used for the fitting. Other traces simply assume the same value for Kd^0 (10.62 ± 0.65 μM). *FRET signal* corresponding to higher-order aggregates is observed for higher peptide concentrations when the DHPC concentration was less than 40 mM. The *inset* presents the evolution of the estimated ΔG of dissociation as a function of micellar detergent concentration. According to the treatment of Fisher et al. (2003), the ordinate and the slope give ΔG^0 at 1 M detergent (28.11 ± 0.65 kJ mol^{-1}) and the susceptibility (-5.65 ± 0.46)

Simulation overview and plan

We carried out a series of simulations (Fig. 2) to study specific aspects of the DHPC–GpAtm PDC structure, energetics, and dynamics. The initial simulation (labeled S24) contained the GpAtm monomer in a micelle of 24 DHPC molecules, spanned 80 ns, and was then extended to 300 ns. In this simulation we analyze the detergent behavior and the peptide's influence on this behavior. We start by studying how distinct detergent populations can form and investigate which parameters distinguish them. We proceed by examining the influence of the peptide on the associated detergent molecules. To determine how the PDC behavior was dependent on the initial structure and thus test the robustness of our results, we realized another simulation, labeled S24R. In this second simulation a configuration was taken after 0.2 ns of simulation S24, and then a large perturbation was applied by rotating the peptide by $\sim 100°$ around its axis with respect to the detergents, then this perturbed structure was allowed to relax over 300 ns. Comparison of simulations S24R and S24 allows us to estimate the robustness of our results.

We also studied the effects of the peptide-to-detergent ratio, and thus indirectly the chemical activity of the detergent. We adopted two different methods to sequentially remove detergent molecules, passing progressively from 24 to 17 monomers. The first strategy consisted in removing detergent monomers with particularly high

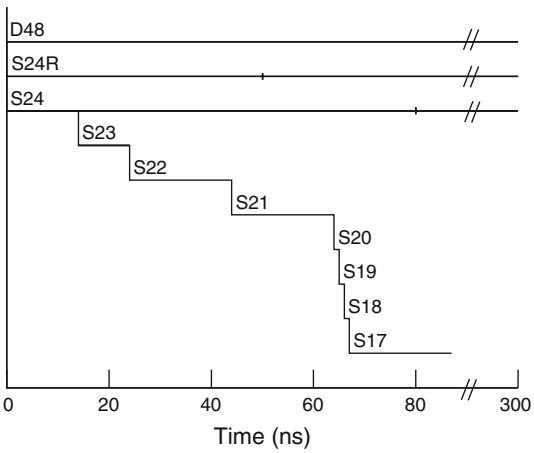

Fig. 2 Summary of the different simulations carried out for this study and their relationships. S24 and S24R are simulations of GpAtm with 24 DHPC molecules that differ in the initial orientation of the peptide within the PDC. S23–S17 are shorter simulations with fewer detergent molecules obtained by successively removing detergent molecules as described in the text. *Dashes* at 80 ns (S24) and 50 ns (S24R) delineate the original simulations and their extensions

detergent–peptide interaction energies. Each removal was followed by 10 or 20 ns of simulation to allow relaxation of the structure (labeled S23–S20). The second strategy consisted in sequentially removing detergent monomers with particularly high detergent–detergent interaction energies with 2 ns of MD simulation for relaxation (labeled S20–S18) and finally a 20 ns MD production run for S17.

Overall structure

Over the 300 ns of simulation S24, the main features of a bilayered micelle, typical of our free DHPC simulation, are conserved (Fig. 3a, c) with some fluctuations that give rise to a more multifaceted micelle. After the 100° rotation of the peptide (simulation S24R), few fluctuations are observed in the general organization of the micelle. The presence of the peptide hardly changes the organization previously observed for our model detergent. In fact, despite the different starting structure, we observed convergence of the two systems (Fig. 3a, b) in the first 80 ns. In the remainder of both simulations, slow relaxation processes that involve reorganization of the detergent molecules around the peptide led to the exposure of the same hydrophobic residues (see below).

Detergent organization

Next, we characterized the interaction network between detergent molecules. To monitor the energetics, we measured the interaction energy of each detergent monomer with the other detergent molecules at the end of the first simulation period (60–80 ns) for the S24 simulation. We define this as the detergent cohesion energy. In Fig. 4 we represent this cohesion energy for all the detergents as a probability density distribution (Fig. 4, black line). A first observation concerns the heterogeneity of the distribution, with some molecules strongly anchored to other detergents and others interacting less strongly. This heterogeneity suggests the existence of several subpopulations. To investigate this we performed a Gaussian deconvolution of the distribution to differentiate the various detergent populations. Three Gaussian components (red, orange, and blue continuous lines) were required to obtain a reasonable fit [black continuous lines, sum of squared residual (SSR) of $\sim 10^{-6}$]. Each of the components are expected to group detergents with similar cohesion energy. The populations obtained are centered at −367.8, −275.2, and −206.3 kJ mol^{-1}. From the relative area of each Gaussian we estimated the number of detergents in each population as 12, 6, and 6 molecules, respectively. To examine more closely our decomposition, we isolated detergent groups with cohesion energies close to the average values estimated from the fitting and of appropriate size, e.g., 12 molecules with cohesion energies near −367.8 kJ mol^{-1}, etc. We then computed the density distribution of these groups of detergent molecules (red, orange, and blue distributions). By comparing the different cohesion energies of the groups and the density distributions resulting from this fitting, we see that the isolated groups effectively correspond to detergent populations. It is worth remarking on the small divergence between the fitting and the distribution on the Gaussian tails, particularly for the population centered at −275.2 kJ mol^{-1}. We attribute this divergence to migration of individual detergent molecules between different populations during the course of the simulation, while they remain associated with a single grouping based on their average cohesion energy. This observation indicates that migration between populations occurs but is relatively slow. As a consequence of the slow reorganization process, the three populations still exist in the last part of the simulation (from 200 to 300 ns) but with a diminution of each energy level of about −25 kJ mol^{-1} (Table 1).

To investigate how different detergent molecules can play distinct roles in solubilizing the peptide, we also studied the mean interaction energy between each detergent molecule

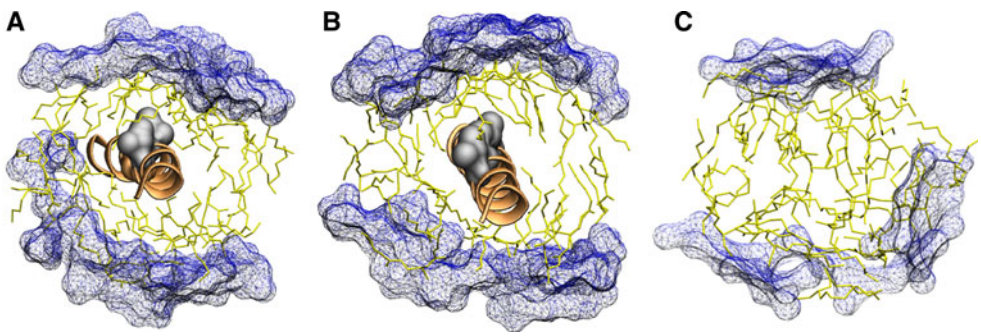

Fig. 3 Structures of the PDC in simulations S24 (**a**) and S24R (**b**), shown at 50 and 80 ns, respectively. For comparison, **c** shows a snapshot of a DHPC micelle. The detergent head-group regions are shown in *blue* and the acyl chains in *yellow*. The polypeptide backbone is shown as a *ribbon* and the valyl ridge as *gray atoms* to aid in visualizing the orientation of the peptide in the PDC and comparison of the structures. All molecular structure diagrams generated using VMD (Humphrey 1996)

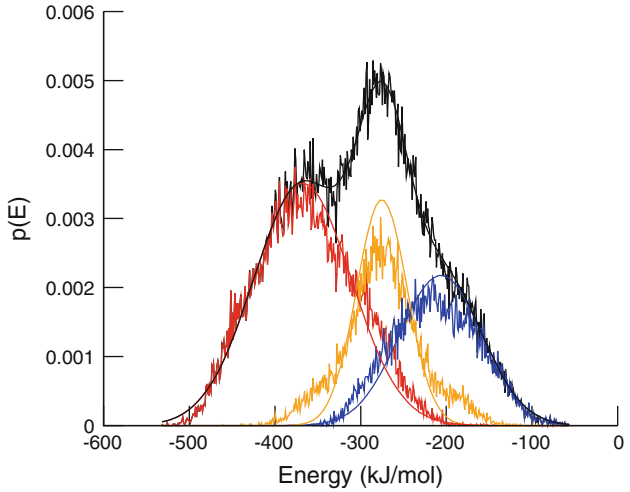

Fig. 4 Detergent cohesion probability density distribution calculated over the 60–80 ns period of the S24 simulation. In *black*: the probability density distribution calculated from the simulations, which was fitted by three Gaussian-distributed subpopulations centered at -367.8 kJ mol^{-1} (*red*), -275.2 kJ mol^{-1} (*orange*), and -206.3 kJ mol^{-1} (*blue*). The probability density calculated for sets of detergent molecules drawn from these distributions was also calculated and is shown using the same color code

and the peptide. This we define as the anchoring energy. Figure 5 shows a three-dimensional view of the complex, where the mean interaction energies are displayed as a color gradient. Figure 5a shows the detergent cohesion energy, and Fig. 5b the detergent anchoring energy. It is clear (Fig. 5a) that detergents in the center of the bilayer patch have dense interaction networks and high cohesion energy, while detergents further from the center have lower cohesion energy. The mean anchoring energy of the detergents (Fig. 5b) shows that, while detergents far away from the peptide are not anchored to it, those close to the peptide have high or intermediate anchoring energy. Comparing the two figures, it is interesting to note that detergents with high cohesion tend to have low to intermediate anchoring. Figure 6a shows the evolution of the detergent anchoring energy distributions as a function of successive simulation periods. It is shown that the distribution is highly heterogeneous, having a significant population with weak anchoring energy (above -10 kJ mol^{-1}) and some population with very strong anchoring energy (between -60 and -150 kJ mol^{-1}). Those energies are mostly due to van der Waals interactions, because electrostatic interactions are very weak. From the first (0–20 ns) to the second period (20–40 ns) the main evolution consists in the diminution of the weak contribution. From 40 to 80 ns the distributions appear more similar and stable; however, some fluctuations that involve medium (-10 to -60 kJ mol^{-1}) and strong anchoring interactions still exist. This shows the existence of slower relaxation processes of the peptide–detergent interactions that are described later.

To further observe how the distinct detergent populations are sensitive to the total number of detergent monomers, we adopted a perturbation strategy, sequentially removing key detergent molecules. The initial detergent-to-peptide ratio we used (i.e., 24) leads to a PDC size similar to pure detergent micelles (Chou et al. 2004; Lin et al. 1986; Tausk 1974). This ratio also corresponds to a detergent mass about twice that of the peptide, as has been experimentally determined for DHPC on diacylglycerol kinase (DAGK) (Vinogradova et al. 1998). However, the PDC size, at a particular detergent chemical activity, should also depend on factors specific to the individual peptide; properties such as surface hydrophobicity are expected to be important (Møller and le Maire 1993). From simulations S24 to S21 we successively removed detergents of highest anchoring energy. The evolution of the distributions is illustrated in Fig. 6b. Importantly, although we removed strongly anchored detergents, the high-energy tail (of strongly fixed detergents) rapidly reforms during

Table 1 Population energetics of detergent cohesion based on the total interaction of each detergent molecule with the remainder of the micelle core

Detergent cohesion population (energy, kJ mol^{-1})				
	Low	Medium	High	SSR
S24[a]	0.26 (-206)	0.24 (-275)	0.50 (-368)	2.09×10^{-5}
S24[b]	0.36 (-231)	0.24 (-302)	0.40 (-393)	4.87×10^{-6}
S24R[b]	0.34 (-231)	0.26 (-302)	0.40 (-393)	4.80×10^{-6}
D48[b]	0.15 (-206)	0.24 (-271)	0.61 (-370)	2.73×10^{-6}

Low, medium, and high correspond to distinct detergent populations obtained by fitting of the distribution of detergent cohesion as obtained in Fig. 3

The size for each population is given, and the corresponding mean energy value in parenthesis (in kJ mol^{-1})

SSR sum of squared residual of fit

[a] Corresponds to a 20-ns interval between 60 and 80 ns, illustrated in Fig. 3

[b] Corresponds to the last 100 ns of the distinct 300-ns simulations

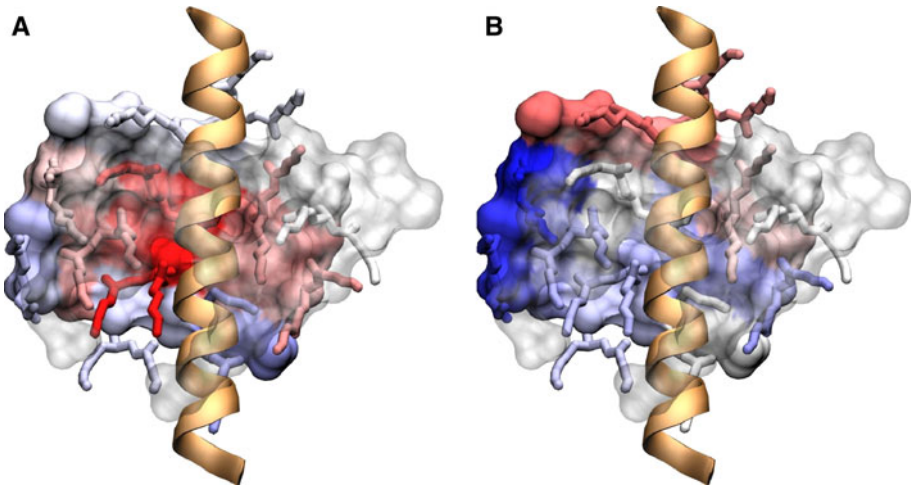

Fig. 5 Mean detergent interaction energies. View of the complex, normal to the top layer of the micelle. The top layer is rendered in *gray*, transparent for visualization, with the peptide in *orange cartoon*. Detergent polar heads are rendered as a surface, and their acyl chains are rendered as sticks. Interaction energies computed over the 60–80 ns period of the S24 simulation are illustrated by a color gradient from *blue* to *red* for weak to strong interactions energies. **a** Detergent cohesion energies. **b** Detergent anchoring energies

relaxation, while the peak due to weakly anchored detergents above -10 kJ mol^{-1} disappears. Thus, as might be expected, the reservoir of poorly anchored detergents can be recruited to occupy a freed site of high interaction potential. When the complex reaches 21 detergents, the intermediately anchored population (8A and 8B, respectively) begins to grow, which is rather unexpected.

The GpAtm helix solvent accessible surface is shown in the helix projections presented in Fig. 7, from which it is apparent that, during this perturbation procedure, the hydrophobic part of the GpAtm peptide remains embedded within the core of the micelle. These projections were made using Ptuba (Lopera et al. 2005); this program unfolds the helix from around its axis and duplicates the surface, allowing simultaneous visualization of all surfaces of the helix. At the structure level it can be observed that, with 21 detergent molecules, only a single layer of detergent contributes to the burial of the hydrophobic surface and thus no more detergent molecule can be removed without affecting the peptide solubility. This was clearly illustrated during the second series of perturbations when weakly anchored detergent molecules were eliminated (S20–S17). This perturbation resulted in draining of DHPC from the valyl-rich face of GpAtm (Fig. 7).

Figure 6b shows the corresponding changes for the evolution of anchoring energy. Not only do the weakly anchored detergents disappear, but upon further depletion the strongly anchored detergents disappear. As a result, the intermediate population grows and shifts to larger anchoring energy, from 25 to 40 kJ mol^{-1}. Even though the detergents are removed far from the valyl ridge on the polypeptide, after relaxation this hydrophobic region of the polypeptide becomes totally exposed to the aqueous solvent. This surprising effect can be rationalized by observing that weakly anchored detergent molecules are often at the center of cohesive interaction networks within the micelle. Thus, the detergent–detergent "cohesion" and the detergent–peptide "anchoring" are not independent and are both important for the structure of the PDC.

Peptide influence on detergent organization

To analyze the effects of the peptide surface on the detergent micelle, we computed the mean interaction energy with detergent for each amino-acyl residue. Figure 8 shows projections of the peptide, color-coded to show mean interaction energies for simulation S24 and S24R (8A and 8B, respectively). Residue interactions are clearly organized along three faces. A first face contains the glycines of the dimerization motif. It has very weak interactions with the detergent (blue). A second face is rich in ramified residues, valines, and isoleucines and has intermediate interactions (white). Finally the red-pink patch is composed of three residues (Tyr, Ala, and Met) that interact very strongly with the detergent.

Thus, it appears that interaction profiles with detergent can be very heterogeneous. Factors such as the side-chain surface area are of importance but do not completely explain the complexity of the interaction potential. Other, more extended, topological considerations such as the ridge created by aligned branched residues or the groove created by aligned glycines have a large influence. Thus, the combination of residues and their local topological environment forms faces that interact differently with the detergent molecules that constitute the environment.

Figure 9 illustrates some representative modes of detergent anchoring to the peptide surface that are associated to particular topologies of the peptide. Detergents anchored to short ramified residues forming a ridge can straddle the ridge while maintaining cohesion (Fig. 9a). Detergents close to the glycine residues do not interact strongly with the polypeptide and show a great variety of flexible conformations (data not shown). Finally, detergents near aromatic residues are strongly adsorbed to the

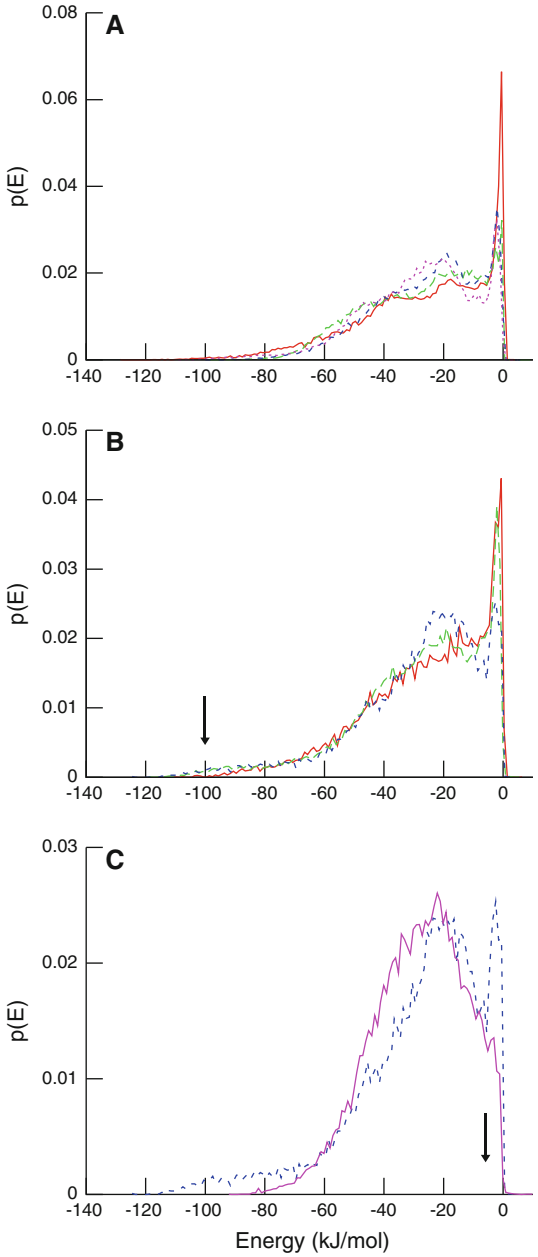

Fig. 6 Evolution of the distribution of anchoring energies. **a** Evolution over four successive 20-ns periods on the first 80 ns of S24 simulation (0–20 *continuous red line*; 20–40 *green long-dashed line*; 40–60 *blue short-dashed line*; 60–80 *magenta dotted line*). **b** Evolution during the first phase (S23–S21) of detergent depletion when successive removals of highly anchored detergents (see *arrow*) finally reduce the number of loosely bound detergent molecules. **c** Illustration of the second phase (S21–S17), during which removal of loosely bound detergent (see *arrow*) causes loss of both tightly and loosely bound detergent (S21 *blue short-dashed line* and S17 *continuous magenta line*)

residue surface and lose their conformation favorable for cohesion (Fig. 9b).

To further characterize the convergence between the two simulations, both were extended until 300 ns. Over this very long time scale, we observed that the two systems continued to evolve as anchoring and cohesion population slowly exchanged, as previously suggested.

As observed in Fig. 10, the peptide accessible surface area continues to evolve over several tens of nanoseconds. It finally settles and fluctuates around 50% of occluded surfaces over the last 100 ns of the simulations. Tables 1 and 2 present the energy distributions for detergent cohesion and peptide anchoring, respectively. The S24 reference interval populations are computed between 60 and 80 ns, when the peptide is fully embedded in the micelle. The last 100 ns of both the S24 and S24R simulations are used to characterize the stabilized PDC, when detergent populations converge to very similar interaction profiles. Through the embedded to exposed peptide transition, the main change is a shift of the three detergent cohesion populations, gaining -25 kJ mol^{-1}, accompanied by a significant decrease of anchoring energies.

As previously observed for smaller peptide–detergent aggregates, the valyl face becomes exposed, while the glycyl region and part of the third face remain buried. This situation (at such peptide-to-detergent ratio) would undoubtedly favor peptide aggregation (and dimerization). A conclusion drawn with this study is that a micelle size close to the experimental aggregation number of DHPC (19 ± 1) may not be enough to solubilize even monomeric GpAtm. Moreover, a gain in detergent cohesion that is not compensated by more favorable interactions with the peptide will favor peptide aggregation.

To investigate whether detergent properties and interaction profiles are modified upon GpAtm dimerization, we also performed a MD simulation of the GpAtm dimer at the same peptide-to-detergent ratio. No changes were observed in the accessible surface of the dimer (Fig. 10) in the course of the whole simulation. The simulation was performed over 300 ns to access the time-averaged quantities given in Tables 1 and 2. The three energy classes obtained from the cohesion profiles resemble those of the early S24 simulation. However, the majority of detergents (>60%) cluster in the high-energy cohesion population. Furthermore, in contrast to what was previously found with the monomer, the anchoring energy between peptide and detergents is stronger on average. The stability of the exposed surfaces and the energy profiles supports the idea that the dimer could be well solubilized in the 48-DHPC complex.

Discussion

Using molecular dynamics simulations, we followed the dynamics of a PDC and studied the different interactions between the various molecules that form the complex.

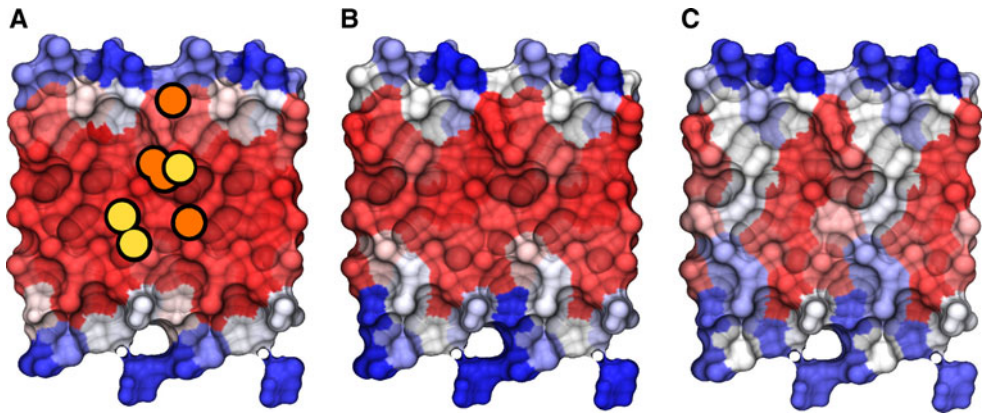

Fig. 7 Accessibility of the peptide, *color-coded* on a Ptuba projection (Lopera et al. 2005) representing the surface of the GpAtm transmembrane helix (see "Materials and methods"): **a** S24 (60–80 ns), **b** S20, and **c** S17 simulations. In each *panel*, accessibility is shown by a *color gradient*, where a fully solvent-accessible residue is *blue*, while a fully buried one is *red*. In S24 and S20, the peptide shows a homogeneous covering all around the peptide's axis, with its terminal residues exposed. In S17, residues along one face of the peptide become exposed, and only a patch of buried residues remains. *Circles* in **a** indicate the position of the strongly (*orange*) or weakly anchored detergent (*yellow*) pulled from the surface of the micelle

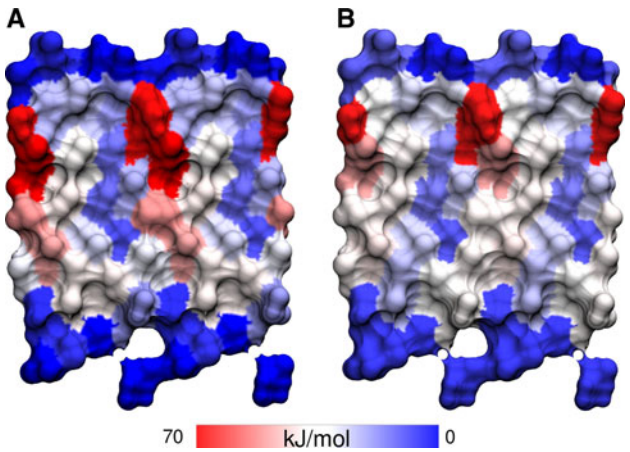

Fig. 8 Interaction energy of the peptide–detergent interaction, *color-coded* on a Ptuba projection (Lopera et al. 2005) representing the surface of the GpAtm transmembrane helix. Energy averaged over the 60–80 ns period of the S24 (**a**) and 30–50 ns period of S24R (**b**) simulations

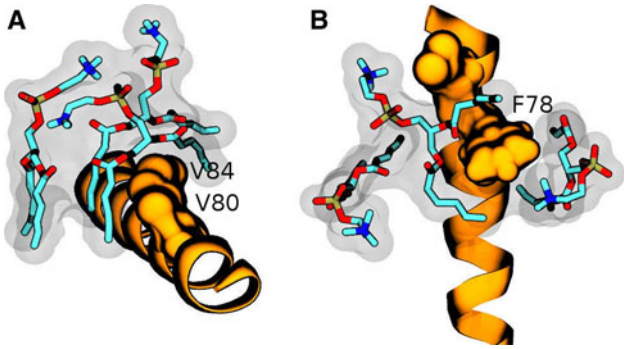

Fig. 9 Representative structures of DHPC. The peptide is colored in *orange*, and lipids in *licorice*. **a** Two detergents straddling the valyl ridge (V80 and V84) are shown, while a third is interacting more weakly with the polypeptide. **b** Two interactions with the phenylalanine residue (F88) are shown where again multiple contacts between the amino acid and each acyl chain of the detergent can be seen

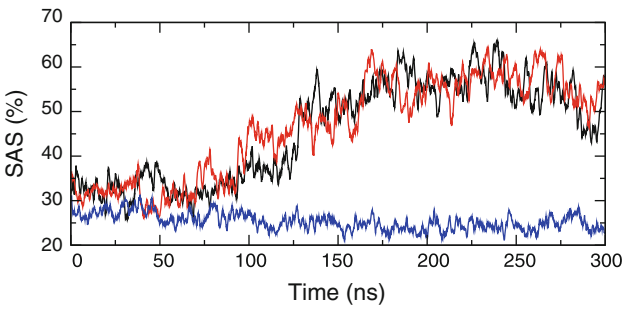

Fig. 10 Evolution of solvent (water) accessible surface for the two monomeric GpAtm peptide simulations, S24 (*black*) and S24R (*red*), and for the dimeric GpAtm simulation, D48 (*blue*). All these simulations were at the same detergent-to-peptide ratio of 24

In the particular system we studied, composed of GpAtm in a DHPC detergent micelle, several previously undescribed structural features can be observed. First, the intermolecular interactions between detergent molecules dictate the supramolecular organization of the micelle; e.g., the bilayered structure that exists in the pure detergent complex is maintained in the presence of the peptide. Second, the orientation of the peptide within this complex is constrained, giving rise to a rigid complex rather than a typical flexible solute–solvent relationship as the result of differential interactions of detergent with the distinct faces of the peptide. It also has consequences for the modulation of peptide association in response to detergent features. Finally, the balance between detergent cohesion and its anchorage to the peptide has effects on peptide solubility. The exposure of the hydrophobic peptide surface to the aqueous phase could explain the limited ability of DHPC to

Table 2 Anchoring populations obtained from individual detergent interaction energies with the GpAtm surface

Detergent anchorage population			
	Strong	Intermediate	Weak
S24[a]	0.06	0.76	0.18
S24[b]	0.10	0.52	0.38
S24R[b]	0.15	0.40	0.45
D48[b]	0.07	0.67	0.26

Based on Fig. 6, detergent–peptide interactions were separated into three distinct populations corresponding to weak (5 to −10 kJ mol^{-1}), intermediate (−10 to −60 kJ mol^{-1}), and strong (−60 to −150 kJ mol^{-1}) interactions. Values are displayed for the GpAtm monomer (S24 and S24R) and for the dimer (D48)

[a, b] See Table 1

solubilize the peptide, as observed in fluorescence measurements. These three aspects are discussed in the following sections.

The association of detergent

In general, insertion of a peptide into a micelle is expected to modify the nature and magnitude of the forces governing the micelle structure. Detergents within the aggregate that could previously reduce their enthalpy only by minimizing the cohesion energy are now required to balance this with the anchoring energy, binding them to the peptide. However, in our model system the interaction between detergent monomers appears sufficient to dictate the general organization of the PDC. The resulting complex retains the essentially bilayered shape that we observed in MD simulations of pure micelles (Fig. 3c). It is important to note that this minimal perturbation may arise from the unexpected orientation of the peptide within the micelle. The short-chain lecithins do not allow the GpAtm to remain in a transbilayer conformation. Though this was the configuration that we originally constructed, it was so unfavorable that the PDC rapidly reorganized to a peptide in the hydrophobic core of the micelle and oriented parallel to the bilayer plane. This illustrates how the magnitude of inter-detergent forces, and consequently the nature of the detergent, may or may not affect the global organization of a complex when peptides or membrane protein are added to micelles. Another consequence of the strong intermolecular interactions is the exposure of the hydrophobic parts of the peptide to the aqueous phase. This situation is relevant to experimental conditions, where the use of low detergent concentrations (or high protein-to-detergent ratio) leads to protein aggregation (Tate 2010). Such conditions can occur in NMR studies of membrane peptides, where such aggregation must be avoided. It has been observed that this tendency varies greatly with the nature of the detergent and possibly with the nature of membrane protein surfaces (Privé 2007; Sanders and Sönnichsen 2006). From our simple model system, it could be observed that the details of the balance between interactions may be a major source of the observed experimental variability. Finally, we suggest that detergents that have strong tendency for cohesion might be prone to this behavior, which, if extrapolated, could be viewed as a phase separation of the transmembrane peptide out of the micelles (Fisher et al. 2003).

Peptide faces

After the cohesion forces between detergent molecules, the anchoring of detergent on the peptide surface is the other key element we examined in our system. This is also of course a key element of experimental membrane protein solubilization. In this context it is hypothesized that a mild detergent should preferentially anchor to the exterior of the protein bundle and that interaction with internal faces should be avoided in order to maintain protein structure and functionality.

For the study of this phenomenon the GpA single transmembrane domain is a particularly useful model system. GpA is a membrane protein found as homodimers in the erythrocyte plasma membrane. Its transmembrane domains is considered as an archetype of α-helix interaction through a GxxxG motif. NMR studies have revealed the structure of the dimeric transmembrane region (residues 63–101) in dodecyl phospho-choline detergent micelles (MacKenzie 1997), and the dimerization motif has been extensively studied (Russ and Engelman 2000). Fluorescence studies from our laboratory have shown the effect of detergent on the dimerization of the helices, and the analysis suggested that the different faces of the helix had different detergent binding properties (Fisher et al. 2003).

In our MD simulations, the particular orientation of the peptide relative to the micelle (parallel to the "pseudo" bilayer) provides an anisotropic environment for the peptide. This leads to considerable heterogeneity in the detergent–peptide interactions. Three peptide faces could be distinguished: the short ramified residue face containing valyl residues from the extended dimerization motif which form a ridge at the surface of the peptide; the glycyl face, which is the core of the canonical GxxxG dimerization motif; and a more heterogeneous face that contains aromatic and longer alkyl chains.

The ridge associated with the first face favors configuration where the bicatenated detergents can straddle the ridge and thus maintain high contact surface for detergent interactions. This structure allows detergents to keep a relatively parallel organization of their fatty acyl chains that allows both anchoring and cohesion to coexist. This topology is expected to have great importance in the

structure of the complex, since it allows the fixing of a whole layer of detergent to the peptide. As we have shown the presence of opposing forces for cohesion and anchoring of the detergents, it seems natural to consider the possible competing forces arising from the peptide topology. While the valyl ridge allows the formation of an anchored layer, the presence of this constraining topology provokes competition with cohesion and thus weakens cohesive forces and could even break the detergent layer. This is observed when the number of detergents is reduced within the PDC and when simulations are performed over a long time scale (300 ns).

The neighboring glycyl-rich face shows a topology that corresponds to a planar surface. In the context of folding and association, this allows the interacting transmembrane helices to pack tightly and the neighboring residues to interact. Since glycine residues lack side-chain, they interact very weakly with the DHPC detergent and impose few constraints on the detergents. Therefore, detergents above this face can maximize their cohesion and maintain the layer organization. Hence, valyl and glycyl topologies seem likely to cooperate in organizing the micelle around the peptide. A detergent that only weakly interacts with an important dimerization motif should be mild and maintain the integrity of the native structure. Also, this is consistent with the experimentally observed behavior of DHPC that classifies this detergent as mild. Our simulations illustrate, at atomic resolution, a behavior often found experimentally: the nature of a detergent modifies the intrinsic capacity of membrane proteins to associate or dissociate. However, the weakness of that interaction comes from both the global and detailed organization of the PDC. Hence, the observation made with our model detergent and model peptide is not necessarily generalizable to other systems. In previous experimental measurements of a series of detergents and GpAtm dimerization we observed that such detergent aggressiveness is not easily correlated to physicochemical parameters of the molecules (Fisher et al. 2003). This corroborates the suggestion that rather specific relationships between protein and detergent are responsible for the empirical scale of aggressiveness. Treating this problem structurally requires more systematic studies of the energetics of various detergents and such topology.

The last, more heterogeneous, face is more difficult to discuss. Some detergents anchor tightly to the peptide, while others seem more dynamic. The layer formed seems to result from a balance between intermediate-cohesion detergents and adhesion to a hydrophobic interface. It seems that the micelle structure results from adaptation of detergents to neighboring and facing detergents rather than to the peptide face. Perhaps most important is the heterogeneity of this face, which prevents a particular organization of the detergent with respect to the amino acids.

Peptide aggregation and solubilization

The detergent organization in a PDC controls the solubility of the resulting complex. In most cases, membrane protein surfaces exposed to lipids are enriched in hydrophobic residues. These residues that are not implicated in the protein structure and function are among the less conserved (Adamian and Liang 2006; Park and Helms 2006). The differences between the coating of different topologies by different detergents could explain the difficulty in finding a rationale for the capacity of detergents to solubilize membrane proteins, even homologous proteins. A neutral substitution at the functional level can have considerable effects on the local surface topology and thus on the way that the region is covered by detergents, with consequences for solubilization and manipulation of the protein.

Likewise, in the coating of the protein by detergents, some faces can be more easily accessible to the solvent. This is particularly critical in experimental conditions typical of structural biology, where the solubilization of a protein as a PDC could occur at minimal detergent-to-protein ratio to avoid excess micelles. We have seen that detergent cohesion can be privileged over peptide coating due to the competitive effects of cohesion and anchoring. Thus, exposure of a hydrophobic face, as observed in our simulations, can occur and provide nonspecific aggregation sites. Remarkably it appears from our simulations that the size of the PDC as assessed by the free micelle aggregation number (20 monomers) does not appear sufficient to properly solubilize even a single GpAtm monomer. This is very relevant to our experimental data showing that DHPC, in contrast to what is observed with other detergents, cannot efficiently solubilize GpAtm until about three times the CMC. Experimentally, aggregation occurs with 10,000-fold molar excess of detergent, showing that a lack of detergent cannot account for this phenomenon. We rather propose that sufficient chemical potential should be present in the detergent solution to allow accommodation of peptides (either monomeric or dimeric) in larger micelles, perhaps resembling the micelle size that solubilizes the dimer in our simulation. This contrasts with a previous simulation of GpAtm dimers in sodium dodecyl sulfate (SDS) showing that micelle sizes half that of the experimental free micelle may be enough to fully solubilize the dimer. However, in the case of SDS as for DHPC a number of detergents between 44 and 55 was used for the PDC (Braun et al. 2004). In the case of the SDS micelle, the GpAtm environment is described as a fluid-like layer of molecules which could rapidly exchange on a 20-ns time scale. This strongly contrasts with our DHPC study that suggests a rigid and constrained complex where changes occur only after drastic micelle structure perturbations and on timescales longer than 100 ns.

Experiments might be useful to probe directly the structural features of the GpAtm–DHPC complex; for example, NMR relaxation measurements on GpAtm in DHPC micelles might characterize the diffusion behavior of the PDC (Chou et al. 2004). Also, fluorescence anisotropy experiments (Coïc et al. 2005; Duneau et al. 1998) applied to labeled peptides together with light scattering measurement might be useful to test the hypothesis that monomer and dimer complexes need more molecules than a simple micelle.

Despite the reasonably good agreement between simulations and the global behavior of DHPC in regard to the GpAtm peptides, some limitation in the modeling methodology should be kept in mind. The high cohesion between DHPC molecules is a consequence of its molecular parametrization in the force field. Here, the corresponding parameters are the same as for the long-chain lecithin (as dimirystoylphospahatidylcholine (DMPC) or dipalmitoylphospahatidylcholine (DPPC)), however any errors in the force field of the lipids (which are still under improvement; Horta et al. 2011) would have consequences, at least at a quantitative level, on the behavior of the DHPC and on its interactions with embedded peptides.

The list of available and fully tested force fields remains limited; however, the extension of these studies to a range of different peptides or proteins solubilized in different detergents will help to identify the hidden and exposed topologies of membrane proteins, and explain how they interact with detergents. In particular, it seems important to investigate the balance between cohesive and anchoring forces. In turn, such study will help describe the relationship between detergent properties and their use in membrane protein studies, and thus could drastically improve the rationalization of membrane protein solubilization, and reduce the wide range of potential detergents for membrane protein solubilization.

Acknowledgments This work was supported by the CNRS and Agence Nationale de la Recherche (ANR). J.K. was supported by a scholarship from the French Ministry of Higher Education and Research (MESR).

References

Adamian L, Liang J (2006) Prediction of transmembrane helix orientation in polytopic membrane proteins. BMC Struct Biol 6:13. doi:10.1186/1472-6807-6-13

Berendsen HJC, Postma JPM, van Gunsteren WF, Hermans J (1981) Interaction models for water in relation to protein hydration. In: Pullman B (ed) Intermolecular Forces. Reidel, Dordrecht, pp 331–338

Berendsen HJC, Postma JPM, van Gunsteren WF, DiNola A, Haak JR (1984) Molecular dynamics with coupling to an external bath. J Chem Phys 81:3684–3690. doi:10.1063/1.448118

Braun R, Engelman DM, Schulten K (2004) Molecular dynamics simulations of micelle formation around dimeric glycophorin A transmembrane helices. Biophys J 87:754–763. doi:10.1529/biophysj.104.040279

Breyton C, Pucci B, Popot J (2010) Amphipols and fluorinated surfactants: two alternatives to detergents for studying membrane proteins in vitro. Methods Mol Biol 601:219–245. doi:10.1007/978-1-60761-344-2¥_14

Chou JJ, Baber JL, Bax A (2004) Characterization of phospholipid mixed micelles by translational diffusion. J Biomol NMR 29:299–308. doi:10.1023/B:JNMR.0000032560.43738.6a

Coïc Y, Vincent M, Gallay J, Baleux F, Mousson F, Beswick V, Neumann J, de Foresta B (2005) Single-spanning membrane protein insertion in membrane mimetic systems: role and localization of aromatic residues. Eur Biophys J 35:27–39. doi:10.1007/s00249-005-0002-1

Darden T, Perera L, Li L, Pedersen L (1999) New tricks for modelers from the crystallography toolkit: the particle mesh Ewald algorithm and its use in nucleic acid simulations. Structure 7:R55–R60. doi:10.1016/S0969-2126(99)80033-1

Dowhan W, Bogdanov M (2009) Lipid-dependent membrane protein topogenesis. Annu Rev Biochem 78:515–540. doi:10.1146/annurev.biochem.77.060806.091251

Drews J (2000) Drug discovery today and tomorrow. Drug Discov Today 5:2–4. doi:10.1016/S1359-6446(99)01428-2

Duneau JP, Garnier N, Cremel G, Nullans G, Hubert P, Genest D, Vincent M, Gallay J, Genest M (1998) Time resolved fluorescence properties of phenylalanine in different environments comparison with molecular dynamics simulation. Biophys Chem 73:109–119. doi:10.1016/S0301-4622(98)00142-2

Duneau J, Vegh AP, Sturgis JN (2007) A dimerization hierarchy in the transmembrane domains of the HER receptor family. Biochemistry 46:2010–2019. doi:10.1021/bi061436f

Duquesne K, Sturgis JN (2010) Membrane protein solubilization. Methods Mol Biol 601:205–217. doi:10.1007/978-1-60761-344-2¥_13

Fernández C, Hilty C, Wider G, Güntert P, Wüthrich K (2004) NMR structure of the integral membrane protein OmpX. J Mol Biol 336:1211–1221. doi:10.1016/j.jmb.2003.09.014

Fisher LE, Engelman DM (2001) High-yield synthesis and purification of an alpha-helical transmembrane domain. Anal Biochem 293:102–108. doi:10.1006/abio.2001.5122

Fisher LE, Engelman DM, Sturgis JN (1999) Detergents modulate dimerization, but not helicity, of the glycophorin A transmembrane domain. J Mol Biol 293:639–651. doi:10.1006/jmbi.1999.3126

Fisher LE, Engelman DM, Sturgis JN (2003) Effect of detergents on the association of the glycophorin A transmembrane helix. Biophys J 85:3097–3105. doi:10.1016/S0006-3495(03)74728-6

Fleming KG (2002) Standardizing the free energy change of transmembrane helix—helix interactions. J Mol Biol 323:563–571. doi:16/S0022-2836(02)00920-8

Garavito RM, Picot D, Loll PJ (1996) Strategies for crystallizing membrane proteins. J Bioenerg Biomembr 28:13–27. doi:10.1007/BF02150674

Hauser H (2000) Short-chain phospholipids as detergents. Biochim Biophys Acta 1508:164–181. doi:10.1016/S0304-4157(00)00008-3

Hess B, Bekker H, Berendsen HJC, Fraaije JGEM (1997) LINCS: a linear constraint solver for molecular simulations. J Comput Chem 18:1463–1472. doi:10.1002/(SICI)1096-987X(199709)18::12<1463:AID-JCC4>3.0.CO;2-H

Horta BAC, Fuchs PFJ, van Gunsteren WF, Hünenberger PH (2011) New interaction parameters for oxygen compounds in the GROMOS force field: improved pure-liquid and solvation properties for alcohols, ethers, aldehydes, ketones, carboxylic acids and esters. J Chem Theory Comput 7:1016–1031. doi:10.1021/ct1006407

Humphrey W (1996) VMD: visual molecular dynamics. J Mol Graph 14:33–38. doi:10.1016/0263-7855(96)00018-5

Kessi J, Poiree J, Wehrli E, Bachofen R, Semenza G, Hauser H (1994) Short-chain phosphatidylcholines as superior detergents in solubilizing membrane proteins and preserving biological activity. Biochemistry 33:10825–10836. doi:10.1021/bi00201a033

Lin TL, Chen SH, Gabriel NE, Roberts MF (1986) The use of small-angle neutron scattering to determine the structure and interaction of dihexanoylphosphatidylcholine micelles. J Am Chem Soc 108:3499–3507. doi:10.1021/ja00272a055

Lopera JA, Sturgis JN, Duneau J (2005) Ptuba: a tool for the visualization of helix surfaces in proteins. J Mol Graph Model 23:305–315. doi:10.1016/j.jmgm.2004.10.004

MacKenzie KR (1997) A transmembrane helix dimer: structure and implications. Science 276:131–133. doi:10.1126/science.276.5309.131

Møller JV, le Maire M (1993) Detergent binding as a measure of hydrophobic surface area of integral membrane proteins. J Biol Chem 268:18659–18672

Park Y, Helms V (2006) How strongly do sequence conservation patterns and empirical scales correlate with exposure patterns of transmembrane helices of membrane proteins? Biopolymers 83:389–399. doi:10.1002/bip.20569

Privé GG (2007) Detergents for the stabilization and crystallization of membrane proteins. Methods 41:388–397. doi:10.1016/j.ymeth.2007.01.007

Rees D, DeAntonio L, Eisenberg D (1989) Hydrophobic organization of membrane proteins. Science 245:510–513. doi:10.1126/science.2667138

Russ WP, Engelman DM (2000) The GxxxG motif: a framework for transmembrane helix–helix association. J Mol Biol 296:911–919. doi:10.1006/jmbi.1999.3489

Sanders CR, Sönnichsen F (2006) Solution NMR of membrane proteins: practice and challenges. Magn Reson Chem 44:Spec No:S24–40. doi:10.1002/mrc.1816

Soares TA, Daura X, Oostenbrink C, Smith LJ, van Gunsteren WF (2004) Validation of the GROMOS force-field parameter set 45Alpha3 against nuclear magnetic resonance data of hen egg lysozyme. J Biomol NMR 30:407–422. doi:10.1007/s10858-004-5430-1

Tate CG (2010) Practical considerations of membrane protein instability during purification and crystallisation. Methods Mol Biol 601:187–203. doi:10.1007/978-1-60761-344-2¥12

Tausk R (1974) Physical chemical studies of short-chain lecithin homologues II micellar weights of dihexanoyl- and diheptanoyl-lecithin. Biophys Chem 1:184–203. doi:10.1016/0301-4622(74)80005-0

Van Der Spoel D, Lindahl E, Hess B, Groenhof G, Mark AE, Berendsen HJC (2005) GROMACS: fast, flexible, and free. J Comput Chem 26:1701–1718. doi:10.1002/jcc.20291

van Gunsteren WF, Berendsen HJ (1984) Computer simulation as a tool for tracing the conformational differences between proteins in solution and in the crystalline state. J Mol Biol 176:559–564. doi:10.1016/0022-2836(84)90177-3

Vinogradova O, Sönnichsen F, Sanders CR (1998) On choosing a detergent for solution NMR studies of membrane proteins. J Biomol NMR 11:381–386. doi:10.1023/A:1008289624496

Wallin E, von Heijne G (1998) Genome-wide analysis of integral membrane proteins from eubacterial, archaean, and eukaryotic organisms. Protein Sci 7:1029–1038. doi:10.1002/pro.5560070420